Eurographics Workshop on 3D Object Retrieval (2017)
I. Pratikakis, F. Dupont, and M. Ovsjanikov (Editors)

Shape Similarity System driven by Digital Elevation Models for Non-rigid Shape Retrieval

Daniela Craciun[1], Guillaume Levieux[2] and Matthieu Montes[1]

[1]Laboratoire GBA, EA4627, Conservatoire National des Arts et Métiers, 2 rue Conté, 75003 Paris, France
[2]Laboratoire CEDRIC, EA4626, Conservatoire National des Arts et Métiers, 2 rue Conté, 75003 Paris, France

Abstract

Shape similarity computation is the main functionality for shape matching and shape retrieval systems. Existing shape similarity frameworks proceed by parameterizing shapes through the use of global and/or local representations computed in the 3D or 2D space. Up to now, global methods have demonstrated their rapidity, while local approaches offer slower, but more accurate solutions. This paper presents a shape similarity system driven by a global descriptor encoded as a Digital Elevation Model (DEM) associated to the input mesh. The DEM descriptor is obtained through the jointly use of a mesh flattening technique and a 2D panoramic projection. Experimental results on the public dataset TOSCA [BBK08] and a comparison with state-of-the-art methods illustrate the effectiveness of the proposed method in terms of accuracy and efficiency.

Categories and Subject Descriptors (according to ACM CCS): Design Methodology [Pattern Recognition]: I.5.1—Pattern analysis

1. Introduction and Motivation

The recent advances in passive and active 3D sensing devices are making available a wide diversity of 3D model repositories [Tri], being increasingly employed for supplying a wide range of civilian and military applications. Their feasibility stands in the capacity to design fast and accurate **S**hape **S**imilarity **S**ystems (**SSS**s) capable to handle a wide range of shape types within massive datasets. Generic benchmarks (**PSB** [SMKF04], **NIST** [FGLW08]) and specialized databases [JKIR06], [BBK08] were built to provide both, datasets variability in presence of shape transformations and evaluation protocols [SMKF04]. Reported methods achieved high recognition rates and key issues shifted towards the scalability aspect [SBS*15]. This requires both: (i) the capability to encode high resolution meshes at coarse level and (ii) similarity measures able to supply fast query search within massive datasets. In our research project, since the shape descriptor is computed only once and stored in a database, we focus on the descriptor comparison runtime for providing a fast query search method.

The present research work proposes a **SSS** designed for performing efficient shape retrieval applications in presence of non-rigid deformations. This paper is organized as follows: the next section reviews representative methods for non-rigid shape retrieval. Section 3 describes the proposed **SSS**, followed by Section 4 which presents experimental results and a comparison w.r.t. state-of-the-art representative methods. Section 5 concludes the present research work and gives main perspectives.

2. Related Work on Non-Rigid Shape Retrieval Systems

This paper focuses on the non-rigid shape retrieval problem which represents a challenging task due to the high number of degrees of freedom detained by flexible shapes. Following the space representation, shape retrieval frameworks can be roughly classified in two categories: methods operating in the 3D space and view-based techniques which exploit 2D representations. For each category, there are shape retrieval systems driven by global and/or local shape signatures.

Geometry-based shape representations providing local descriptors such as Spin Images [JH99] and Shape Context [KPNK03] provide invariance to rigid motion, while MeshHOG (Histogram of Gradients) [ZBVH09] demonstrated robustness to non-rigid deformations. Pose-invariant methods relying on Laplace-Beltrami spectrum were also introduced, such as ShapeDNA [RWP06] and Global Point Signature [Rus07]. Local features based on Laplace-Beltrami operator include Heat Kernel Signature [SOG09] and Wave Kernel Signature [ASC11]. They provide an effective solution for invariance to non-rigid deformations. A recent survey on spectral methods can be found in [LBH14]. Visual-similarity shape retrieval systems proceed by generating multiple 2D projections (silhouettes, depth-buffer) and by measuring the similarity via different shape descriptors [CTSO03], [PPTP10]. As stated in [LGS10], most of view-based methods rely on pose normalization performed before projection generation. In addition, the shape similarity is computed over multiple projections, making them unsuitable for large corpus datasets. In order to decrease computational

DOI: 10.2312/3dor.20171051

time, recent research works are directed towards feature-coding approaches aimed at designing a more compact shape representation. Reported methods include Shape Google [BBGO11] which applies the Bag-of-Features (BoF) paradigm [OCZ07] to spectral descriptors [LBH14]. Other techniques combine Multidimensional Scaling and BoF [LGSZ10], [LGS10], or apply geodesic distance [MS05] to local extremas followed by clustering [TDVC11]. Supervised approaches based on sparse coding [LBH15] and deep learning [FXD*15] have also reported effective results.

The present research work combines a mesh flattening shape representation with a 2D panoramic projection to encode the Digital Elevation Model (DEM) associated to the input mesh. The performances of the DEM descriptor used jointly with global dissimilarity metrics are studied for supplying shape retrieval applications in presence of non-rigid deformations.

3. Proposed Shape Similarity System

The proposed system is composed of two main stages: (i) the global descriptor computation and (ii) the shape comparison stage which are described through the present section.

Representing shapes as Digital Elevation Models. The present work exploits the DEM concept traditionally employed in cartography for representing Earth's surface from terrain elevation data [ML58]. In the surface representation processing block, the input mesh is encoded as a DEM through the use of a two-steps projection. The algorithm starts by applying the mesh flattening procedure introduced in [AHTK99] which maps the input mesh, noted $\mathcal{M}$, onto the unit sphere using the Laplace-Beltrami operator [GGS03]. The spherical mapping provides a valid solution for any genus-0 triangle meshes, being adapted in our current research work. In addition, mapping the surface on the unit sphere introduces inevitable distortions which we plan to evaluate and compensate in our future work.

In the second step, the unit sphere is projected onto a 2D spherical panoramic grid and the elevation values of the input mesh are assigned to each 2D grid location. The generation of 2D panoramic view proceeds by converting the point cloud $\mathbf{P}_S$ associated to the flatten mesh in spherical coordinates (θ, φ, ρ). The converted points are further injected into a $2D$ Delaunay triangulation procedure [Sch96] in order to compute the intrinsic parameters of the spherical projection, namely the angular steps $(\delta\theta, \delta\varphi)$ and the spherical field of view given by $[\theta_{\min}, \theta_{\max}] \times [\varphi_{\min}, \varphi_{\max}]$. In order to handle spherical mappings with variable angular steps estimates, we generate a square grid with constant angular resolution $\delta\widetilde{\theta} = \delta\widetilde{\varphi} = 0.01$. A 3D point on the unit sphere is mapped onto the 2D grid space through the projection $\mathcal{P}$:$\mathbf{R}^3 \rightarrow \mathbf{R}^2$ expressed as:

$$\mathcal{P}(\theta_i, \varphi_i, \rho_i) \rightarrow \mathbf{m}(u_i, v_i) \quad (1)$$

where, $\mathbf{m}(u_i, v_i) = p_{z,i}, i = 1, .., N_p$, represents the 2D grid location storing the elevation value, p_z, of the associated 3D point $\mathbf{p} = (p_x, p_y, p_z) \in \mathcal{M}$, with N_p denoting the number of vertices present in the input mesh $\mathcal{M}$. The final output is the DEM associated to the input mesh $\mathcal{M}$, defined as $E = \{(u, v, p_z)(i), i = 1, ..., N_p\}$. This results in a global descriptor which encodes shape's elevation, while providing topology and fast comparison over a 2D grid space. Figure 1 illustrates an overview of the DEM descriptor computation procedure. In our research work we studied the invariance of the proposed DEM descriptor under rigid transformations and scale variations applied to the input mesh. The DEM descriptor is stable under rotations and translations variations of the input mesh and varies in presence of scale transformations. In addition, in our experiments we observed that the overall mapping distortions (mesh flattening and 2D grid projection) subject to the level of detail present in the mesh, may give rise to a certain invariance limits w.r.t. the rigid motion magnitude and to the mesh resolution. For this reason, the isometry invariance must be evaluated w.r.t. input mesh types in order to draw the conditions in which the invariance property is preserved.

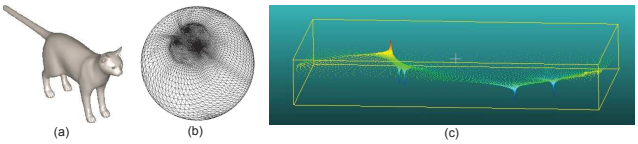

Figure 1: *Overview of the DEM descriptor computation procedure on an input mesh belonging to the TOSCA dataset [BBK08]: (a) input mesh: cat ♯0, (b) spherical mapping [AHTK99] obtained for the input mesh cat ♯0, (c) DEM output corresponding to the input mesh illustrated in Figure(a), color code: elevation values.*

Global comparison of DEMs. The shape similarity is computed by comparing the DEMs associated to the query and target meshes through the use of global distance measures. The present research work evaluates the Mean Absolute Differences ($d_{MAD}(u, v, p_z)$) and the Root Mean Square Deviation ($d_{RMSD}(u, v, p_z)$) distances. For input meshes with different number of points, distances are computed over the minimum number of common points (noted N_{min} and computed between the query and the target meshes). In absence of scale variations, the comparison measures a valid similarity when shapes belonging to the same class result in DEM with similar size. Figure 2 illustrates an example of the shape similarity output generated by the $d_{MAD}(u, v, p_z)$ distance on a query belonging to the TOSCA dataset [BBK08]. It can be observed that the query search resulted in true positives (TP). In addition, Figure 2 emphasize that the dissimilarity score is also able to quantify the amplitude of local deformations and thus, to rank the progressively less similar targets according to the query. The proposed **SSS** compares one descriptor per shape, while providing an explicit surface representation which gives the possibility to recover information about the areas corresponding to non-rigid deformations.

4. Experimental Results and Performance Evaluation

Dataset. The TOSCA dataset [BBK08] was chosen for assessing the performances of the proposed system. While being a small dataset, it allows analysing in detail the algorithm's behaviour for problem identification. The dataset is composed of 80 models belonging to 9 classes. For each class, a different number of targets are available as true positives.

Evaluation measures. The retrieval performances of the proposed framework are studied by employing the evaluation protocol introduced in [SMKF04] which measure the Nearest Neigh-

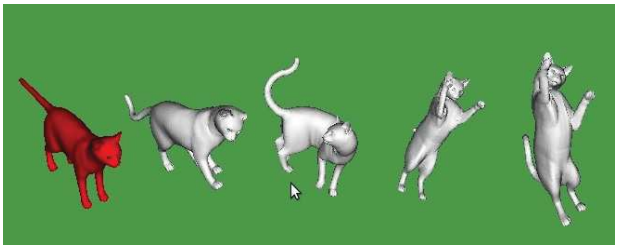

(a)

Figure 2: *Shape similarity output generated by the $d_{MAD}(u,v,p_z)$ distance on an input mesh belonging to the TOSCA dataset [BBK08]: (a) red color - query, white color: best $N = 4$ best targets output.*

bor (NN), First Tier (FT), Second Tier (ST), Mean Average Precision (MAP) and the Precision-Recall graphs. The evaluation was made based on the source codes released for SHREC'15 contest [SBS*15], which focused on the scalability of non-rigid shape retrieval algorithms.

Comparison to State-of-the-Art. We selected top-ranked techniques evaluated on both, non-rigid shapes retrieval benchmarks [LGB*13], [LZC*15] and large scale generic datasets [LLL*15], including non-rigid shapes. The first evaluated technique, ShapeDNA [RWP06], belongs to spectral methods. As in [BK10], the evaluation was done by selecting the first 15 eigen values. The all-vs-all dissimilarity matrix is computed using the L_2 distance computed between feature vectors associated to each shape. The second evaluated method is a view-based technique, PANORAMA [PPTP10], which has reported effective results on the latest large scale benchmark [LLL*15], containing also non-rigid shapes. The third evaluated method is the Viewpoint Feature Histogram (VFH) [RBTH10] employed for object and pose recognition. It relies on points' normal computation and encodes each shape in a 308-bins histogram. The Sum of Absolute Differences (SAD) is selected for computing the dissimilarity measure between histograms.

Accuracy evaluation. From Figure 3 it can be observed that top-rank methods include ShapeDNA and the proposed DEM descriptor employed along with $d_{RMSD}(u,v,p_z)$ and $d_{MAD}(u,v,p_z)$ distances. Lower recognition rates correspond to the view-based method, PANORAMA, and to the VFH descriptor. When analyzing the retrieval performances illustrated in Table 1, it can be observed that ShapeDNA and the proposed method, $d_{MAD}(u,v,p_z)$, generated similar performances, except for the ST measure.

Shape comparison runtime. Algorithms were evaluated on a 64b machine equipped with an Intel Xeon running at 2.3 GHz and with 32Gb of RAM memory. The proposed algorithm is implemented in C/C++ and relies on PCL [RC11], VTK [WSL06] and ITK libraries. Table 2 illustrates the runtime obtained for computing the similarity score for the same input mesh, cat ♯0. Computation time shows that histogram-based techniques (ShapeDNA, VFH) provide the fastest comparison, while PANORAMA is the most computationally expensive approach. The proposed 2D grid-based method bridges the gap between the evaluated histogram-based and view-based methods.

Table 1: *Accuracy evaluation measures for each compared method.*

RecRate(%)	NN	FT	ST	MAP
$d_{RMSD}(u,v,p_z)$	**0.95**	0.7960	0.7525	0.8373
$d_{MAD}(u,v,p_z)$	0.9375	**0.8123**	**0.7795**	**0.8653**
$SAD[VFH]$	0.7625	0.5429	0.5664	0.6132
PANORAMA	0.7125	0.4479	0.3338	0.503
shapeDNA	**0.9625**	**0.8226**	**0.9157**	**0.88851**

Table 2: *Runtime (seconds) for computing the similarity score for the query cat♯0.*

Method (♯ bins)	CPU (s)
$d_{RMSD}(u,v,p_z)$	$32.8e-5$
$d_{MAD}(u,v,p_z)$	$23e-5$
SAD[VFH] (308)	$56e-7$
PANORAMA	$12e-3$
shapeDNA (15)	$6e-7$

Although ShapeDNA exhibits competitive running time, the presented DEM descriptor provides an explicit shape representation suitable for identifying, although with an approximation, areas corresponding to non-rigid deformations. In addition, the dissimilarity score allows to quantify the amplitude of non-rigid deformations and thus, to rank the progressively less similar targets according the query.

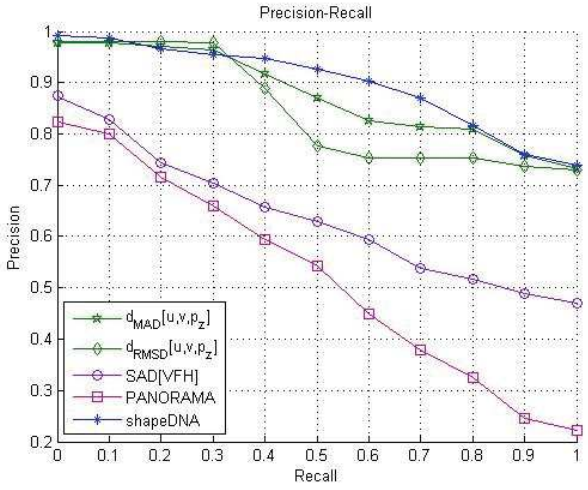

Figure 3: *Precision-Recall plots for each compared method.*

5. Conclusions and Research Perspectives

This paper presented a global shape descriptor encoded as a Digital Elevation Model designed for supplying fast query search for shape retrieval applications in presence of non-rigid deformations. Main perspectives of the present research work are concerned with

the extension of the proposed descriptor to larger datasets (higher genus surfaces) and deformations types. Future work is also directed towards the optimization onboard parallel processing units.

Acknowledgements. The present research work is supported by the ERC ViDOCK Grant no. ♯640283 from the European Research Council Executive Agency.

References

[AHTK99] ANGENENT S., HAKER S., TANNENBAUM A., KIKINIS R.: On the Laplace-Beltrami operator and brain surface flattening. *IEEE Transactions on Medical Imaging 18*, 8 (Aug 1999), 700–711. 2

[ASC11] AUBRY M., SCHLICKEWEI U., CREMERS D.: The wave kernel signature: A quantum mechanical approach to shape analysis. *ICCV Workshops* (2011), 1626–1633. 1

[BBGO11] BRONSTEIN A. M., BRONSTEIN M. M., GUIBAS L. J., OVSJANIKOV M.: Shape Google: Geometric words and expressions for invariant shape retrieval. *ACM Trans. Graph. 30*, 1 (2011). 2

[BBK08] BRONSTEIN A. M., BRONSTEIN M. M., KIMMEL R.: Numerical geometry of non-rigid shapes. *Springer* (2008). 1, 2, 3

[BK10] BRONSTEIN M. M., KOKKINOS I.: Scale-invariant heat kernel signatures for non-rigid shape recognition. *In Proc. Int. Conf. on Computer Vision and Pattern Recognition* (2010), 1704–1711. 3

[CTSO03] CHEN D.-Y., TIAN X.-P., SHEN Y.-T., OUHYOUNG M.: On visual similarity based 3D model retrieval. *Computer Graphics Forum* (2003). 1

[FGLW08] FANG R., GODIL A., LI X., WAGAN A.: A new shape benchmark for 3D object retrieval. *Advances in Visual Computing: 4th International Symposium, ISVC 2008, Las Vegas, NV, USA, December 1-3, 2008. Proceedings, Part I* (2008), 381–392. 1

[FXD*15] FANG Y., XIE J., DAI G., WANG M., ZHU F., XU T., WONG E.: 3D deep shape descriptor. *The IEEE Conference on Computer Vision and Pattern Recognition (CVPR)* (June 2015). 2

[GGS03] GOTSMAN C., GU X., SHEFFER A.: Fundamentals of spherical parameterization for 3D meshes. *ACM SIGGRAPH 2003 Papers* (2003), 358–363. 2

[JH99] JOHNSON A., HERBERT M.: Using Spin Images for efficient object recognition in cluttered 3D scenes. *In IEEE Trans. on Pattern Analysis and Machine Intelligence* (1999). 1

[JKIR06] JAYANTI S., KALYANARAMAN Y., IYER N., RAMANI K.: Developing an engineering shape benchmark for CAD models. *Computer-Aided Design 38*, 9 (2006), 939–953. 1

[KPNK03] KORTGEN M., PARK G. J., NOVOTNI M., KLEIN R.: 3D shape matching with 3D shape contexts. *In the 7th Central European Seminar on Computer Graphics* (2003). 1

[LBH14] LI C., BEN HAMZA A.: Spatially aggregating spectral descriptors for nonrigid 3D shape retrieval: A comparative survey. *Multimedia Syst.* (2014). 1, 2

[LBH15] LIU Z., BU S., HAN J.: Locality-constrained sparse patch coding for 3D shape retrieval. *Neurocomputing* (2015), 583–592. 2

[LGB*13] LIAN Z., GODIL A., BUSTOS B., DAOUDI M., HERMANS J., KAWAMURA S., KURITA Y., LAVOUÉ G., VAN NGUYEN H., OHBUCHI R., OHKITA Y., OHISHI Y., PORIKLI F., REUTER M., SIPIRAN I., SMEETS D., SUETENS P., TABIA H., VANDERMEULEN D.: A comparison of methods for non-rigid 3D shape retrieval. *Pattern Recogn. 46*, 1 (Jan. 2013). 3

[LGS10] LIAN Z., GODIL A., SUN X.: Visual similarity based 3D shape retrieval using bag-of-features. *2010 Shape Modeling International Conference* (2010), 25–36. 1, 2

[LGSZ10] LIAN Z., GODIL A., SUN X., ZHANG H.: Non-rigid 3D shape retrieval using Multidimensional Scaling and Bag-of-Features. *2010 IEEE International Conference on Image Processing* (2010), 3181–3184. 2

[LLL*15] LI B., LU Y., LI C., GODIL A., SCHRECK T., AONO M., BURTSCHER M., CHEN Q., CHOWDHURY N. K., FANG B., FU H., FURUYA T., LI H., LIU J., JOHAN H., KOSAKA R., KOYANAGI H., OHBUCHI R., TATSUMA A., WAN Y., ZHANG C., ZOU C.: A comparison of 3D shape retrieval methods based on a large-scale benchmark supporting multimodal queries. *Computer Vision and Image Understanding 131* (2015), 1 – 27. Special section: Large Scale Data-Driven Evaluation in Computer Vision. 3

[LZC*15] LIAN Z., ZHANG J., CHOI S., ELNAGHY H., EL-SANA J., FURUYA T., GIACHETTI A., GULER R., ISAIA L., LAI L., LI C., LI H., LIMBERGER F., MARTIN R., NAKANISHI R., NETO A., NONATO L., OHBUCHI R., PEVZNER K., PICKUP D., ROSIN P., SHARF A., SUN L., SUN X., TARI S., UNAL G., WILSON R.: Shrec 15 track: Non-rigid shape retrieval. *In Eurographics Workshop on 3D Objects Retrieval* (2015). 3

[ML58] MILLER C. L., LAFLAMME R. A.: The digital terrain model - theory and application. *Photogrammetric Engineering* (1958), 433–442. 2

[MS05] MEMOLI F., SAPIRO G.: A theoretical and computational framework for isometry invariant recognition of point cloud data. *Foundations of Computational Mathematics*, 5 (2005), 313–346. 2

[OCZ07] O. CHUM J. PHILBIN J. S. M. I., ZISSERMAN A.: Total recall: Automatic query expansion with a generative feature model for object retrieval. *In Proc. Int. Conf. on Computer Vision (ICCV)* (2007). 2

[PPTP10] PAPADAKIS P., PRATIKAKIS I., THEOHARIS T., PERANTONIS S.: PANORAMA: A 3D shape descriptor based on panoramic views for unsupervised 3D object retrieval. *International Journal of Computer Vision 89*, 2 (2010), 177–192. 1, 3

[RBTH10] RUSU R. B., BRADSKI G. R., THIBAUX R., HSU J. M.: Fast 3D recognition and pose using the Viewpoint Feature Histogram. *IEEE International Conference on Robotics and Intelligent Systems* (2010), 2155–2162. 3

[RC11] RUSU R. B., COUSINS S.: 3D is here: Point Cloud Library (PCL). *IEEE International Conference on Robotics and Automation (ICRA)* (2011). 3

[Rus07] RUSTAMOV R. M.: Laplace-Beltrami eigenfunctions for deformation invariant shape representation. *Proceedings of the Fifth Eurographics Symposium on Geometry Processing* (2007). 1

[RWP06] REUTER M., WOLTER F.-E., PEINECKE N.: Laplace-Beltrami spectra as Shape-DNA of surfaces and solids. *Computer-Aided Design 38*, 4 (2006), 342–366. 1, 3

[SBS*15] SIPIRAN I., BUSTOS B., SCHRECK T., BRONSTEIN A. M., BRONSTEIN M., CASTELLANI U., CHOI S., LAI L., LI H., LITMAN R., SUN L.: Scalability of non-rigid 3D shape retrieval. *In Proc. Eurographics Workshop on 3D Object Retrieval (3DOR)* (2015), 121–128. 1, 3

[Sch96] SCHEWSHUK J. R.: Triangle: Engineering a 2D quality mesh generator and Delaunay triangulator. *In Applied Computational Geometry: Toward Geometric Engineering 12*, 1148 (1996), 203–222. 2

[SMKF04] SHILANE P., MIN P., KAZHDAN M., FUNKHOUSER T.: The Princeton shape benchmark. *Shape Modeling International* (2004). 1, 2

[SOG09] SUN J., OVSJANIKOV M., GUIBAS L.: A concise and provably informative multi-scale signature based on heat diffusion. *Proceedings of the Symposium on Geometry Processing* (2009), 1383–1392. 1

[TDVC11] TABIA H., DAOUDI M., VANDEBORRE J.-P., COLOT O.: Deformable shape retrieval using bag-of-feature techniques. *Proc. SPIE 7864* (2011). 2

[Tri] TRIMBLE: 3dwarehouse. *https://3dwarehouse.sketchup.com/*. 1

[WSL06] W. SCHROEDER K. M., LORENSEN B.: The visualization toolkit. *Third Edition Kitware Inc.* (2006). 3

[ZBVH09] ZAHARESCU A., BOYER E., VARANASI K., HORAUD R.: Surface feature detection and description with applications to mesh matching. *In Proc. IEEE Conf. on Computer Vision and Pattern Recognition* (2009). 1